atmosphere

MDPI

Article

Influence of Natural Tropical Oscillations on Ozone Content and Meridional Circulation in the Boreal Winter Stratosphere

Tatiana Ermakova [1,2,*], Andrey Koval [1], Kseniia Didenko [1,3], Olga Aniskina [2] and Arina Okulicheva [2]

[1] Atmospheric Physics Department, Saint Petersburg University, 7/9 Universitetskaya Nab., St. Petersburg 199034, Russia; a.v.koval@spbu.ru (A.K.); didenko.xeniya@yandex.ru (K.D.)
[2] Department of Meteorological Forecasts, Russian State Hydrometeorological University, 79 Voronezhskaya Ulitsa, St. Petersburg 192007, Russia
[3] Pushkov Institute of Terrestrial Magnetism, Ionosphere and Radio Wave Propagation, Russian Academy of Sciences (IZMIRAN), 4 Kaluzhskoe Hw., Moscow 108840, Russia
* Correspondence: taalika@mail.ru

Abstract: The dependence of ozone content in the polar stratosphere upon different phases of the quasi-biennial oscillation (QBO) of the zonal wind and the El Niño–Southern Oscillation (ENSO) during winter was studied. The monthly (from November to January) mean residual meridional circulation (RMC) was calculated for four different combinations of the main phases of ENSO and QBO using MERRA2 reanalysis data. It has been demonstrated that the QBO phase manifests itself in different vertical distributions of ozone in the equatorial stratosphere, as well as in strengthening/weakening of the secondary meridional circulation in the tropics. The enhancement of the RMC from the tropical to the polar stratosphere is stronger at altitudes where ozone is higher in the tropics under El Niño conditions. The RMC modification and intensification are observed from ozone-depleted areas under La Niña conditions. A "cumulative" effect is observed by February under La Niña conditions and the easterly QBO, which is expressed in the lowest ozone content in the polar stratosphere. The numerical experiments carried out using the Middle and Upper Atmosphere Model (MUAM) confirmed tendencies in changes in the meridional transport detected from the reanalysis data for different combinations of QBO and ENSO.

Keywords: stratospheric ozone; residual meridional circulation; El Niño–Southern Oscillation; quasi-biennial oscillation

Citation: Ermakova, T.; Koval, A.; Didenko, K.; Aniskina, O.; Okulicheva, A. Influence of Natural Tropical Oscillations on Ozone Content and Meridional Circulation in the Boreal Winter Stratosphere. *Atmosphere* **2024**, *15*, 717. https://doi.org/10.3390/atmos15060717

Academic Editor: Yoshihiro Tomikawa

Received: 23 March 2024
Revised: 3 June 2024
Accepted: 11 June 2024
Published: 15 June 2024

1. Introduction

The state of the ozone layer has recently attracted increased attention due to changes in its global content [1,2], as well as an understanding of the role of ozone not only as a protector of life on Earth from the harmful effects of hard ultraviolet solar radiation but also as a factor influencing climate and the whole biosphere [3]. Ozone can be considered as an indicator of thermal and chemical imbalance in the Earth–atmosphere system. Most of the ozone (about 90%) is found in the stratosphere. Minor changes in the ozone content in this layer affect dynamic, chemical, and radiation processes in the atmosphere and climate forecasts in general. Many studies have noted an increase in total ozone after the mid-1990s since the adoption of the Montreal Protocol and its Amendments and Adjustments on the protection of the ozone layer and the reduction of concentration of halogenated ozone-depleting gases [4]. However, in recent decades, there has also been an increase in chlorine-containing chemicals, which impede the restoration of ozone in the stratosphere [5–7]. The expected future recovery of stratospheric ozone is now being questioned due to both the observed increase in ozone-depleting gases and the mismatch between predictions of numerical models and measured data [8–12].

Ozone is mainly formed in the tropical stratosphere as the solar insolation is the highest over the tropics, which is necessary for photodissociation reactions. Atmospheric

meridional circulation redistributes ozone to the middle and high latitudes, where it sinks and accumulates in the stratosphere. Ozone concentration is low in the troposphere. It increases sharply above the tropopause, reaching a maximum in the lower stratosphere, between 15 and 25 km in winter at high latitudes and between 25 and 30 km in the tropics. An ozone enhancement near the tropopause is observed due to a rise in the frequency of stratospheric–tropospheric ozone exchange. This sharp increase in concentration, in turn, affects the total ozone content and its ground-level concentration [13–16]. Above 30 km altitude, ozone concentration decreases exponentially with altitude but less rapidly than air density. This slower decrease in ozone concentration explains why the maximum ozone mixing ratio is observed at higher altitudes than that of maximum ozone concentration.

The ozone content in the Polar Regions has seasonal dependence: minimum concentrations are present in winter and maximum concentrations in summer. Antarctica experiences an ozone hole every winter, while ozone holes are less common over the Arctic. The low ozone content in the winter polar stratosphere is associated with the absence of solar radiation during the polar night and the formation of the stratospheric polar vortex. In winter, significant meridional temperature gradients between the tropics and the poles in the stratosphere lead to the formation of strong westerly winds (the polar night jet). The air inside this circle of winds becomes increasingly colder, and strong winds prevent the mixing of polar and tropical air masses, which leads to the formation of an ozone hole.

The ozone variability and its connection with mean meridional circulation in the stratosphere in both hemispheres in different months is investigated in numerous studies (e.g., [17,18]). It is noted that weak meridional circulation with low polar stratospheric temperature leads to polar ozone depletion. Since the process of stratospheric polar vortex development is not identical each autumn, ozone variability in early January could be concerned with the thermodynamics in the stratosphere [19]. From the point of view of remote sensing, the polar stratosphere is a complex object of study. Polyakov et al. [20] showed that low signal and small vertical temperature gradients significantly increase the errors in satellite ozone determinations. To increase the accuracy of satellite sensing, the highest quality a priori information is used—modeling and reanalysis data. Thus, modeling of dynamic processes in the polar stratosphere becomes an important aspect of the current research.

Tropical oscillations, such as the El Niño–Southern Oscillation (ENSO) and the quasi-biennial oscillation (QBO) of the equatorial zonal wind in the stratosphere, as well as solar cycles and volcanic activity, influence regional and global circulations, thus impacting the state of the stratospheric polar vortex in winter over the Arctic through teleconnections [21]. ENSO is generated by the interaction of the ocean and the atmosphere in the tropical Pacific. Positive temperature anomalies in the eastern or central equatorial Pacific associated with El Niño (the positive phase of ENSO) reduce the typically large sea surface temperature difference in the tropical Pacific. Trade winds weaken as a result, the Southern Oscillation index becomes anomalously negative, and sea level falls in the west and rises in the east as warming progresses [22,23]. La Niña is the opposite (negative) phase of the Southern Oscillation relative to El Niño, with unusually low pressure west of the date line and high pressure—east during periods of abnormally low equatorial Pacific sea surface temperatures. ENSO is one of the most important climate events on Earth due to its ability to alter global atmospheric circulation, which, in turn, influences temperature and precipitation across the globe [24].

Observations, as well as the results of numerical experiments, show that the stratospheric polar vortex is warmer and more disturbed under conditions of a positive ENSO phase [20]; the situation is the opposite during a cold phase [25]. The activity of stationary planetary waves with the zonal wave number 1 (SPW1) is higher in the stratosphere and weaker at middle latitudes at the stratospheric jet maximum region during El Niño's mid-winter. The modeled and observed SPW2 amplitude behaves in the opposite way and is larger in the stratosphere during La Niña. The observed changes in SPW1 and SPW2 amplitudes under La Niña and El Niño events should affect the potency of the stratosphere–

troposphere coupling, and the influence of stratospheric processes on circulation patterns in the troposphere can be evinced in different longitudinal sectors [26].

The QBO manifests itself in the tropical stratosphere as a change in the direction of the zonal wind with an average period of 28 months, which also has a significant impact on the global atmospheric circulation. The QBO is characterized by alternating westerly and easterly wind regimes, the boundary between which gradually moves down from the middle stratosphere to the lower one. The QBO influences the width and location of extratropical waveguides along which planetary waves (PWs) propagate from the troposphere to the upper atmosphere [27]. It is assumed that during the boreal winter, the polar vortex under the easterly QBO phase (EQBO) is weaker and more disturbed than under the westerly phase (WQBO) due to PWs' activity increase. These data were also confirmed recently using numerical simulations [27]. PWs spread disturbances from the QBO into high latitudes and the upper atmosphere, including the thermosphere, while propagating in different ways along modified waveguides [28].

A growing number of works are dedicated to studying the joint influence of QBO and ENSO on atmospheric and oceanic processes. The authors of the investigation [29] considered the joint influence of the stratospheric QBO and ENSO on the polar vortex, subtropical westerly jets, and wave patterns during boreal winter. They showed the strengthening of the stratospheric polar vortex during the westerly phase of the QBO and also that the manifestation of the QBO in the stratosphere is stronger under La Niña conditions [30]. They also examined the combined influence of ENSO and QBO on the relationship between sea ice extent and Eurasian climate in winter through planetary wave activity and the stratospheric polar vortex. They note that warm winters are observed in Europe, mostly under La Niña and easterly QBO. Under these conditions, the propagation of planetary waves from the troposphere to the stratosphere is weaker, which leads to a strengthening of the stratospheric polar vortex.

In this study, based on the Merra2 reanalysis data [31], the joint influence of QBO and ENSO phases on the global meridional circulation and, as a consequence, on the transport of stratospheric ozone from low to high latitudes is considered. The main goal of the study is to demonstrate the relationship between the phases of tropical atmospheric ocean oscillations and changes in global ozone content in the extra-tropical stratosphere during the boreal winter, including the possible formation of ozone holes. To verify the conclusions obtained from the reanalysis, a number of numerical calculations of atmospheric circulation were also carried out using the MUAM (Middle and Upper Atmosphere Model) for various QBO/ENSO combinations.

2. Materials and Methods

MERRA-2. In order to study the ENSO-QBO influence on RMC and ozone content in the polar stratosphere during boreal winter, we use "Modern-Era Retrospective analysis for Research and Applications, version 2" (MERRA-2) [31]. The data cover the time interval from 1980 to the present with a spatial resolution of $0.5^\circ \times 0.625^\circ$ and a time step of 3 h. The vertical pressure scale is ranging from 1000 to 0.1 hPa. MERRA-2 also provides an ozone mass mixing ratio, which is assimilated from different sources (the solar backscatter ultraviolet SBUV; Microwave Limb Sounder on Aura satellite; ozone parameterization in GEOS-5 by Rienecker et al. [32]).

MERRA2 data are widely used to study atmospheric ozone variability (see, e.g., [33–38]). The main advantages of these data are their spatial and temporal homogeneity, as well as the duration. The quality of MERRA2 ozone data has also been checked many times (see, e.g., [33,35]). In particular, good agreement was demonstrated between the reanalysis and satellite data on the ozone mixing ratio in the stratosphere. There may be some discrepancy in the upper stratosphere, which is likely due to the simplified parameterization of ozone chemistry used in MERRA2 [33,34]. However, possible ozone biases will not prevent us from documenting the relative trends observed in ozone during different QBO/ENSO phases. We conducted an additional study comparing ozone distributions

for individual years and months with MLS data. Unfortunately, satellite data do not cover all the years we selected for the study. The comparison results demonstrate the overall similarity between the reanalysis data and satellite data for the mean zonal ozone mixing ratio averaged for considered months (Figures 1, S1 and S2).

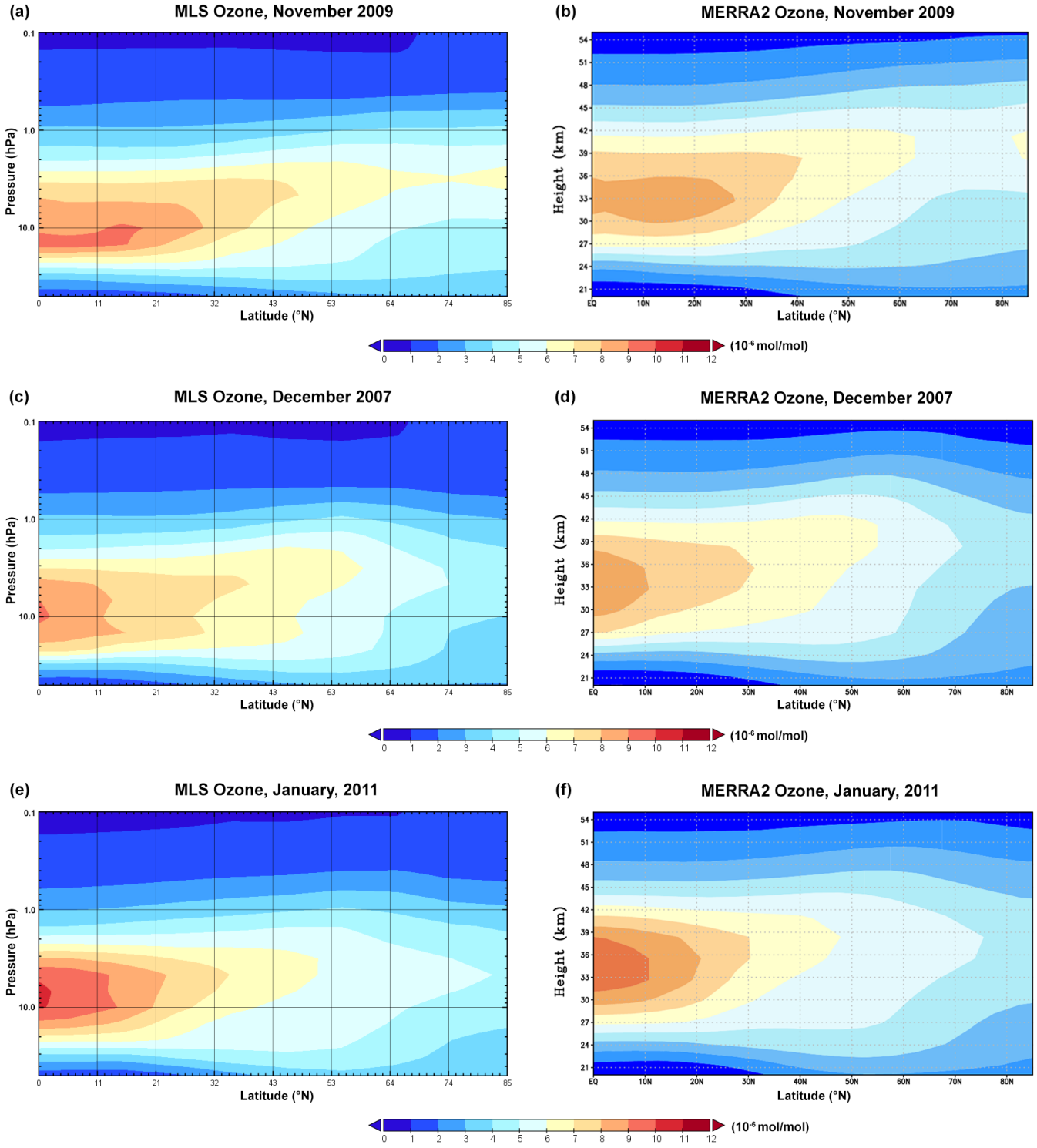

Figure 1. Mean zonal ozone mixing ratio (MLS, (**a**,**c**,**e**)) (MERRA2, (**b**,**d**,**f**)), averaged for November 2009 (**a**,**b**), December 2007 (**c**,**d**), and January 2011 (**e**,**f**).

ENSO phases. The MEI.v2 index (https://psl.noaa.gov/enso/mei/ accessed on 28 May 2023) was used to define the ENSO phase. This index incorporates oceanic (ocean sur-

face temperature) and atmospheric (sea level pressure, zonal and meridional components of surface wind, and outgoing long-wave radiation) variables. The tropical Pacific Ocean (30° S–30° N and 100° E–70° W) is the area for the index calculations. The index is calculated using natural orthogonal functions (NOFs) over rolling two-month time intervals to account for the seasonality of ENSO and reduce the impact of higher frequency intraseasonal oscillations. When considering winters under positive ENSO phase conditions, the El Niño type (canonical or Modoki) [39] was not taken into account due to the fact that the available data do not allow us to collect a sufficient number of winters under different combinations of QBO and ENSO for research.

QBO phases. To determine QBO phases, we use the decomposition of observed equatorial zonal wind variations (JRA55 reanalysis) with empirical orthogonal functions (EOFs) in the altitude range of 1–70 hPa. The QBO signal at these heights is decomposed into two main EOFs. Their scattering diagram is subdivided into 4 patterns, which can be interpreted as the QBO phases. This approach was described in [28]. Employment of the EOFs provides the ability to take into account the spacio-temporal evolution of QBO in order to minimize possible uncertainties in the determination of the QBO phases caused usually by choosing the altitude of the zonal wind observation. A similar approach to defining QBO phases was used earlier; see, e.g., [40]. This approach was applied to the longest time series of data on meteorological parameters on a regular grid to date—the Japanese reanalysis JRA-55 [41]. Zonal wind anomalies were considered relative to the period 1958–2022, previously smoothed using a moving average with an averaging window of five months. The seasonal trend has been removed. Data were considered at nine isobaric levels (70, 50, 30, 20, 10, 7, 5, 3, and 1 hPa).

Residual mean meridional circulation. It is known that using the approach within the framework of the usual Eulerian mean meridional circulation (with zonal averaging of meridional and vertical circulation flows), wave sources of momentum and heat are compensated by advective ones in the dynamic equations [42,43]. This property makes it difficult to analyze the wave effect on the mean flow. Compensation of wave and advective flows in the Eulerian approach also occurs in the continuity equation for long-lived gas components, and thus, the use of the Eulerian mean meridional circulation is ineffective for calculating their transport [44]. To overcome this shortcoming, this study uses the transformed Eulerian mean circulation approach first introduced in [45]. This approach makes it possible to diagnose the wave effect on the mean flow and also provides the ability to calculate the processes of trace gas transport in the meridional direction. It is based on consideration of the so-called mean residual meridional circulation (RMC), which is a combination of eddy and advective mean transport. The following formulas were used to calculate the meridional and vertical components of the RMC:

$$\overline{v}^* = \overline{v} - \frac{1}{\partial\overline{\theta}/\partial z}\left(-\frac{\overline{v'\theta'}}{H} + \frac{\partial\overline{v'\theta'}}{\partial z} - \frac{\overline{v'\theta'}}{\partial\overline{\theta}/\partial z}\frac{\partial^2\overline{\theta}}{\partial z^2}\right). \quad (1)$$

$$\overline{w}^* = \overline{w} + \frac{1}{a\cos\varphi}\frac{1}{\partial\overline{\theta}/\partial z}\left(-\sin\varphi\overline{v'\theta'} + \cos\varphi\left(\frac{\partial\overline{v'\theta'}}{\partial\varphi} - \frac{\overline{v'\theta'}}{\partial\overline{\theta}/\partial z}\frac{\partial^2\overline{\theta}}{\partial z\partial\varphi}\right)\right). \quad (2)$$

where the overbars denote zonal-mean values, the primes indicate deviations from the zonal-mean values; v and w—meridional and vertical wind components; z—vertical coordinate; θ—potential temperature; φ—latitude; and a is the radius of the Earth. A detailed description of the RMC concept and methodology used for its calculating is presented in [46].

Ozone mixing ratio. The evolution of ozone fields was examined using MERRA2 reanalysis data. Boreal winter seasons were selected for the study, taking into account different combinations of QBO and ENSO phases (see Table 1). Three winter seasons were chosen for each combination. This small number of winters is caused by the limited time series of reanalysis data in the satellite era. Distributions of the average ozone mixing

ratio in the stratosphere (from 18 to 40 km) of the Northern Hemisphere were presented for different combinations: El Niño and westerly QBO (El-WQBO), El Niño and easterly QBO (El-EQBO), La Niña and westerly QBO (La-WQBO), and La Niña and easterly QBO (La-EQBO) for November, December, January, and February. The indirect influence of the phases of tropical oscillations on the transport of ozone from low latitudes should appear more clearly at the beginning of the cold period in November and December. This is because sudden stratospheric warmings (SSWs) that can have a significant impact on the stratospheric dynamics of high and mid-latitudes are not so often observed in these months. Modern observations indicate that polar ozone concentrations increase during SSWs, especially during major SSWs with reversal of the zonal wind [47–49]. However, certain transport patterns caused by some combination of QBO and ENSO may produce a cumulative effect. High-latitude stratospheric ozone, for example, may vary little in early winter despite the presence of SSWs in December and the first half of January.

Table 1. Winters under different ENSO and QBO phases.

Phases	El Niño	La Niña
WQBO	1982–1983 1992–1993 1994–1995	1998–1999 2007–2008 2010–2011
EQBO	1986–1987 2002–2003 2009–2010	1999–2000 2011–2012 2017–2018

Numerical simulation. To carry out numerical simulations of the general atmospheric circulation, the MUAM model was used. This is a finite-difference nonlinear mechanistic model capable of reproducing atmospheric circulation at altitudes from the Earth's surface to 300–400 km with a time step of 2 h and a spatial resolution of 5.625° × 5°. The vertical grid consists of 56 nodes. A detailed description of the model is presented in [50]. Features of the numerical experiment, taking into account the QBO phases based on the nudging procedure, are described in [51]. The inclusion of ENSO phases in the MUAM is specified by parameterizing heating due to latent heat release in the equatorial lower stratosphere [26]. To improve statistical significance, ensembles of model runs were calculated for each of the QBO-ENSO combinations, consisting of 10 runs.

3. Results

Figure 2 shows the horizontal distribution of the average ozone content (ozone mass mixing ratio) in the stratosphere (18–40 km) according to the MERRA2 reanalysis data for each month from November to February for four combinations of QBO and ENSO (average for three years shown in Table 1). In Figure 2, we show the average ozone distribution integrated throughout the stratosphere because the ozone changes in the polar stratosphere can vary differently at various altitudes during sudden stratospheric warmings. The left column in Figure 2 shows the horizontal ozone distribution for the La Niña-EQBO combination, which we chose as basic as far as the ozone transport is the weakest under La Niña-EQBO conditions. Further, we show differences in ozone content, temperature, and RMC between other combinations and the La Niña-EQBO. Hence, positive anomalies, presented in all panels except the left column, show ozone increase under all conditions relative to La Niña-EQBO for every month. We subtract the La Niña-EQBO combination from three other ones as the ozone transport is the smallest under La Niña-EQBO conditions. It is easier to see with positive mean zonal ozone anomaly (red shading) at mid and high latitudes. Each combination is represented by averaging over a set of three years, indicated in Table 1.

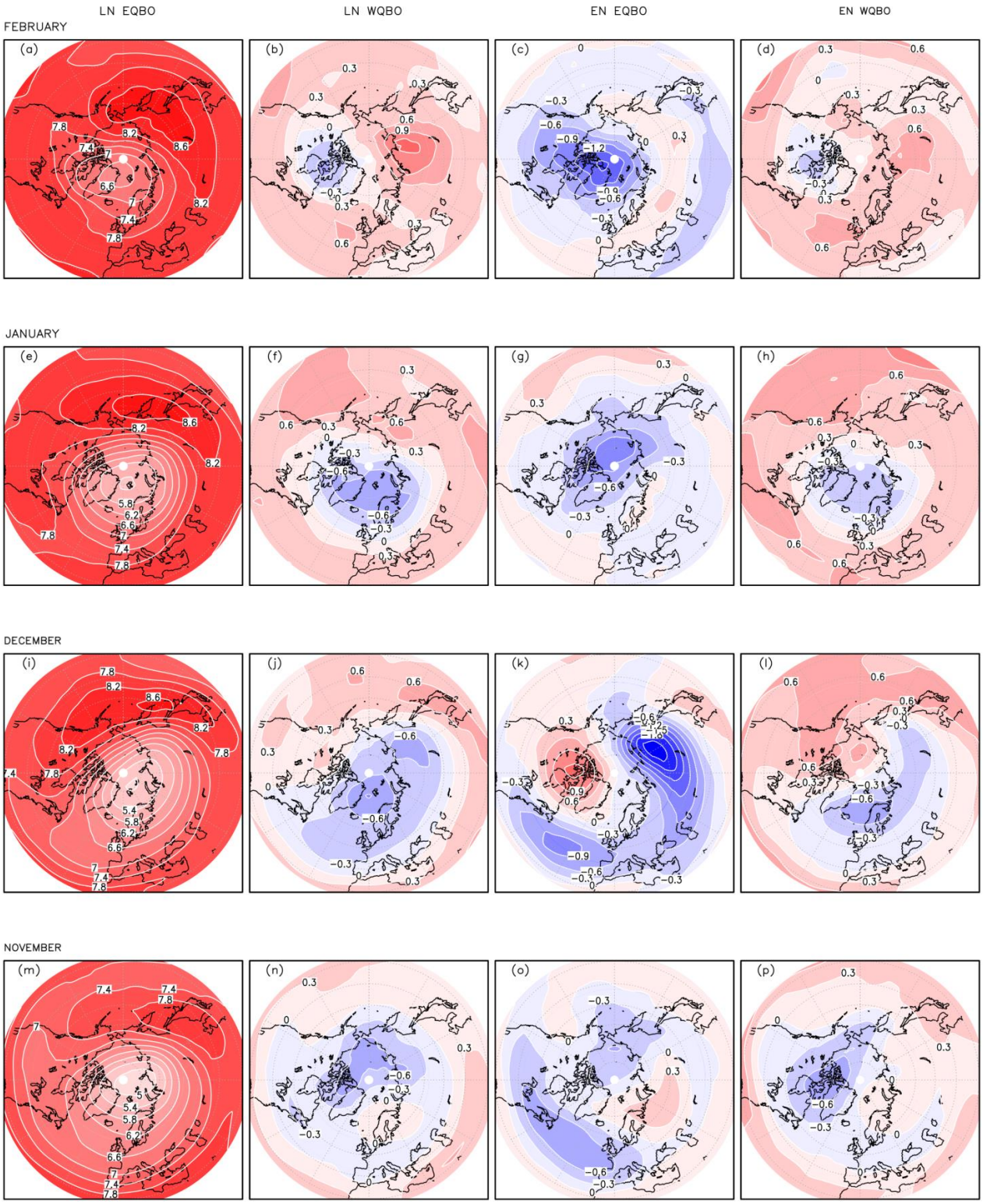

Figure 2. Mean ozone mixing ratio (kg/kg 10^6) for three winter seasons under La Niña-EQBO (left column) and the difference between La Niña-EQBO and other combinations: La Niña-WQBO (second column, El Niño-EQBO (third column), and El Niño-WQBO (right column) in November (**m**–**p**), in December (**i**–**l**), in January (**e**–**h**), and in February (**a**–**d**).

In November, minimum values of the ozone mixing ratio are observed under La Niña-EQBO conditions over the North Pole, Canada, and the Far East; positive increments are shown for other combinations (Figure 2n–p). The changes are of the order of 10%. Minimum

ozone over Europe and Russia is shown during El Niño-EQBO (Figure 2o). In December, two "cores" of positive anomalies are shown during El Niño-EQBO (Figure 2k), which are caused by the reaction of the stratospheric polar vortex to a sharp temperature increase for more than 25 K and the planetary wave activity in the second half of December 2002. This temperature rise was not accompanied by the reversal of the zonal wind component, while its speed dropped almost to zero m/s at the end of the month, forming a minor SSW event. In general, for all combinations in Figure 2j–l, we see an increase in ozone content over Eurasia and the Atlantics relative to La Niña-EQBO (Figure 2i).

In January, similar behavior can be seen for both combinations with the westerly QBO; there is an increase in ozone over the North Atlantic and Europe compared to the easterly QBO (Figure 2f,h). The difference between the ENSO phases (Figure 2d,e) can be explained by the impact of SSWs: in years with El-Niño, SSWs are stronger, and their influence, expressed in an increase in ozone content, is more noticeable. In February, the differences in overall ozone trends associated with the QBO, same as in January, are also pronounced. Only the latitudinal sectors have changed.

Changes in Residual Mean Circulation (RMC), temperature, and ozone content were also analyzed for various months and ENSO-QBO combinations. Figures 3–5 show the latitude–altitude distributions of the three-year average RMC, zonal mean ozone content, and temperature for the La Niña-EQBO combination, as well as the difference between other combinations and La Niña-EQBO for November (Figure 3, an individual figure for RMC for different event combos – Figure S3), December (Figure 4, an individual figure for RMC for different event combos – Figure S4), and January (Figure 5).

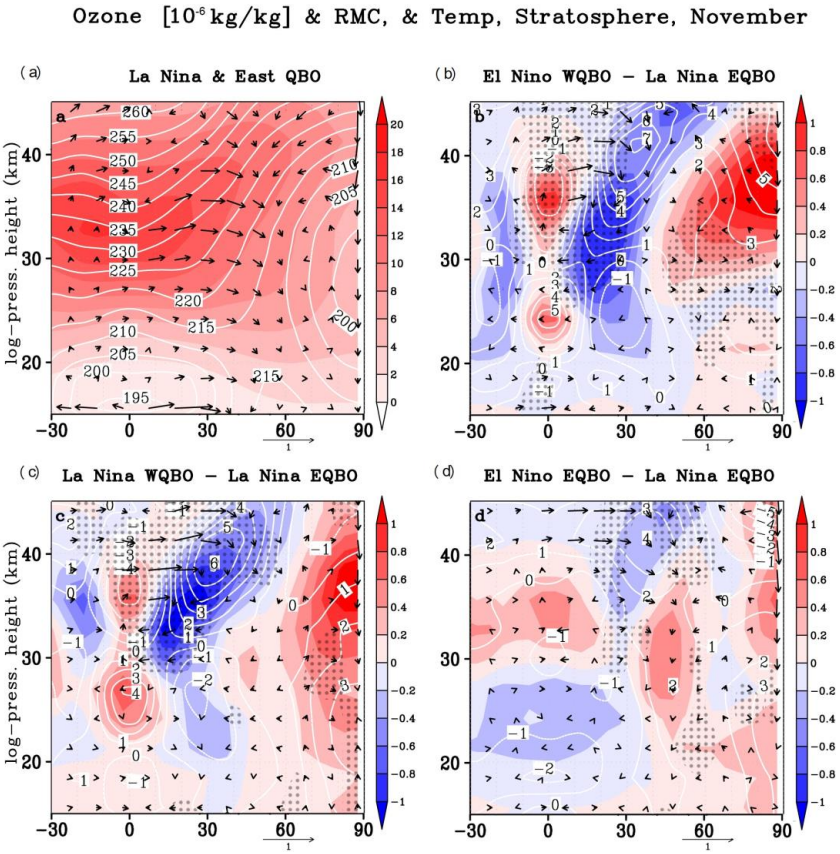

Figure 3. Mean zonal ozone mixing ratio during La Niña-EQBO (**a**) and the difference between La Niña-EQBO and other combinations (**b**–**d**)—shading, mean RMC (**a**), and its increments (**b**–**d**)—arrows, mean zonal temperature (**a**), and its difference (**b**–**d**)—contours in November. Dotted areas reveal statistically significant differences in RMC and temperature at 95%. The vertical component is multiplied by 100 (in sm/s).

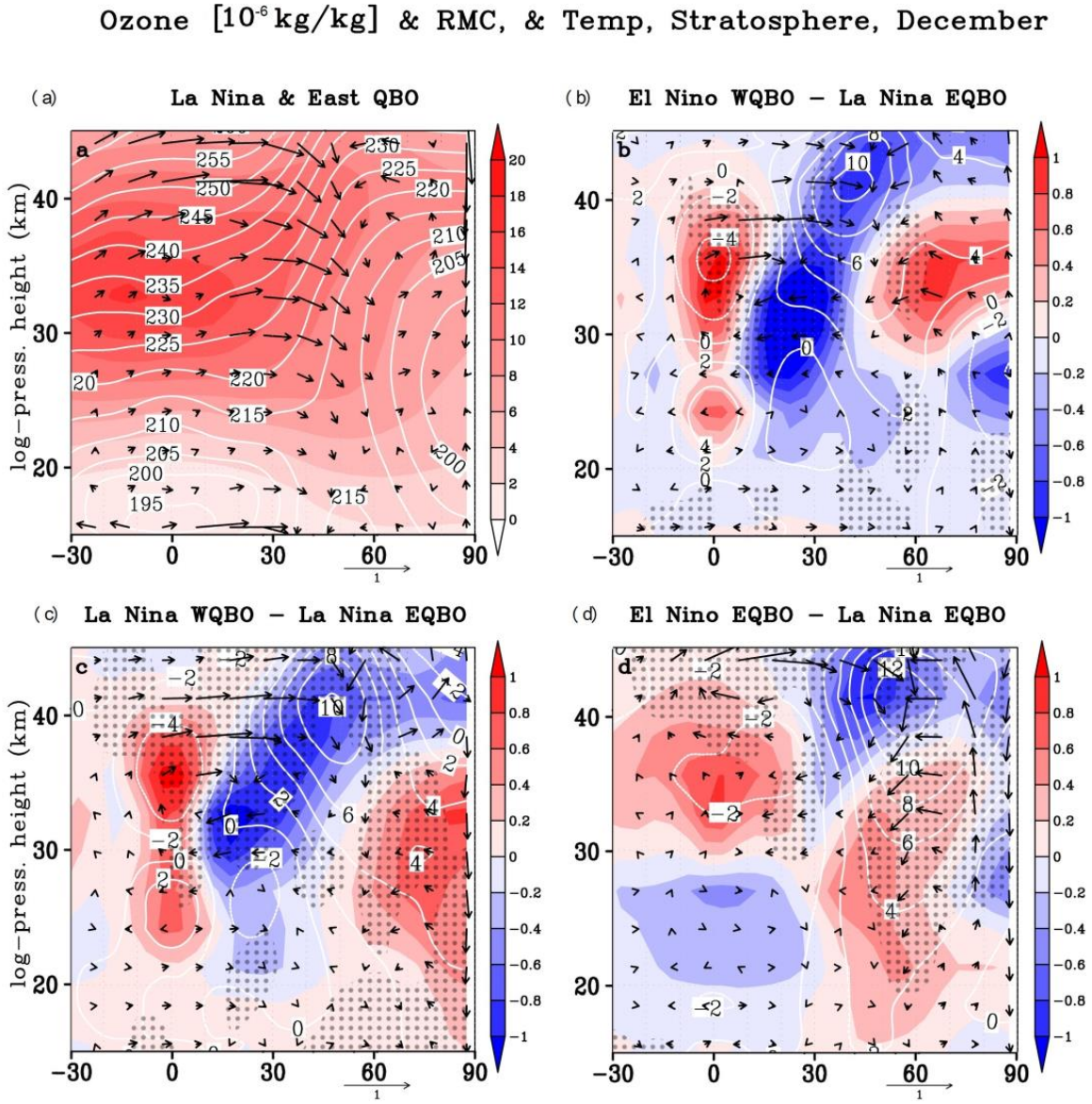

Figure 4. Mean zonal ozone mixing ratio during La Niña-EQBO (**a**) and the difference between La Niña-EQBO and other combinations (**b**–**d**)—shading, mean RMC (**a**), and its increments (**b**–**d**)—arrows, mean zonal temperature (**a**), and its difference (**b**–**d**)—contours in December. Dotted areas reveal statistically significant differences in RMC and temperature at 95%. The vertical component is multiplied by 100 (in sm/s).

Figure 3 shows that stratospheric ozone exhibits the effect of different QBO phases above the equator, which is manifested in the increased ozone content in the lower stratosphere during WQBO (panels b and c). This negative anomaly during EQBO is associated with large vertical movement from low ozone concentration areas, which is confirmed by previous studies [52,53]. The difference is most substantial at an altitude of 25 km. At about 30 km, this difference is less obvious, and the second maximum is noted at an altitude of 35 km. The temperature anomaly at the heights of the two maximums (25 and 35 km) reaches 5 degrees, with the opposite signs in the lower and upper stratosphere. In Figure 3d, we observe a slight decrease in ozone during El Niño relative to La Niña up to an altitude of 30 km and the opposite situation above 30 km in the equatorial stratosphere in the case of the same QBO phase. It is obvious that both chemical and dynamic factors influence the distribution of ozone in the tropical stratosphere since both the temperature anomaly and the vertical transport of NOx caused by the QBO play important roles here. However,

scientists continue to debate the extent to which the chemical processes associated with the QBO influence ozone anomalies [53–55].

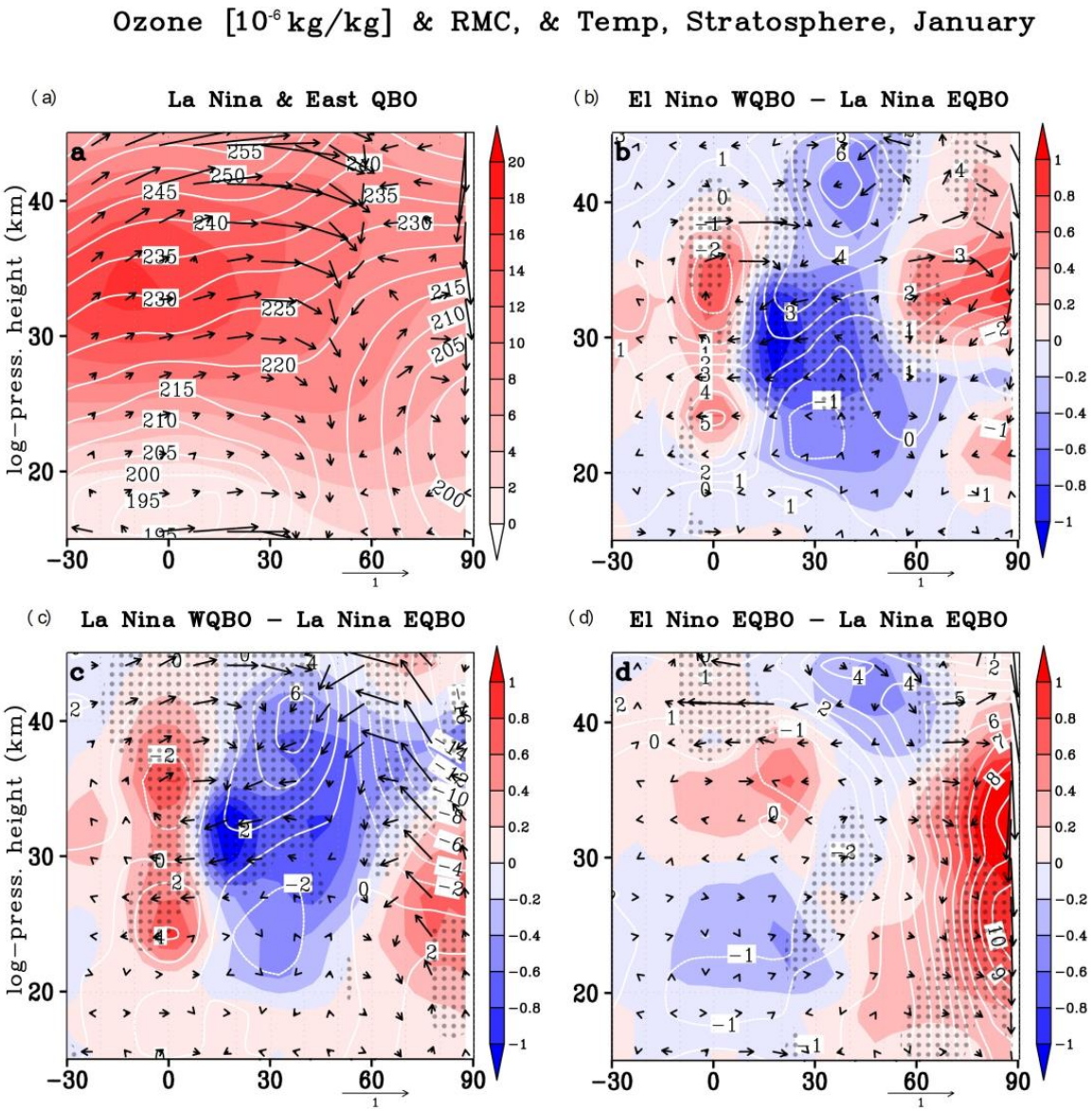

Figure 5. Mean zonal ozone mixing ratio during La Niña-EQBO (**a**) and the difference between La Niña-EQBO and other combinations (**b**–**d**)—shading, mean RMC (**a**), and its increments (**b**–**d**)—arrows, mean zonal temperature (**a**), and its difference (**b**–**d**)—contours in January. Dotted areas reveal statistically significant differences in RMC and temperature at 95%. The vertical component is multiplied by 100 (in sm/s).

The statistical significance of the increments of RMC and temperature was calculated using a paired Student's *t*-test based on data of three years for each combination, taking into account a 3-hour time step. The dots in Figures 3–5 depict the areas where the temperature increments and the OMC component are significant by 95%, and for ozone changes, we calculated the significance separately so as not to overload Figures 2–4. This significance is demonstrated in Figures S5–S7 in Supplementary Materials.

The manifestation of the QBO in the ozone content between 15° and 25° N is opposite in phase to the manifestation in the equatorial belt (10°S–10°N). The border between the two modes is located at 10–15° in both hemispheres [56]. This boundary is obvious in Figure 3b,c and is associated primarily with the QBO phase. The negative increment in RMC

during the WQBO at this boundary at an altitude of 28–33 km indicates enhanced transport in this area during the EQBO. An increase in transport during the WQBO is observed at altitudes of 35 km and above, just from the region of the second ozone maximum increment at the equator. This type of transfer may indirectly explain the higher ozone content over the pole in November during the WQBO (Figure 2n,p) relative to the EQBO. The observed RMC and temperature anomalies shown in Figure 3b,c, leading to changes in ozone content in the equatorial and tropical regions, are explained by the influence of the secondary meridional circulation, which is induced by the QBO [57] (Figure 3) and [58]. In particular, as shown in the work of Ribera et al. [59], such secondary meridional circulation cells are characterized by adiabatic heating/cooling due to vertical movements in areas of zonal wind shear, causing corresponding temperature anomalies.

The region with the minimum content of ozone in the stratosphere is observed under La Niña-EQBO conditions in December (Figure 2i). The location of the region with the minimum ozone content can be influenced by SSW. The stratospheric polar vortex stretches or shifts from its original position and weakens during warming. Ozone-rich air from lower latitudes reaches the pole, causing ozone concentrations to increase. A major SSW with an increase in temperature to 25 K and a reversal of the zonal wind component occurred in early January in the winter of 2011–2012. However, an initial increase in temperature and a weakening of the zonal wind component, which are inherent to SSW, were observed in the second half of December. Obviously, in this case, the ozone content is expected to be higher under La Niña-EQBO conditions (Figure 2i) compared to El Niño-EQBO and WQBO (Figure 2k,l). Under the latter combinations' conditions, SSW was not observed in December in any winter. In such cases, the vortex, as a rule, intensifies, and its temperature decreases, but the ozone content does not change. The dipole of positive increments in Figure 2k is likely caused by high wave activity in mid-December 2002, which led to a shift in the stratospheric polar vortex. Warming with the reversal of the zonal wind component and with an increase in the zonal mean temperature above 30 K was observed in December during the La Niña-WQBO winter of 1998–1999. This is indirectly confirmed by the negative values in Figure 2j over the Arctic Ocean and the highest temperature increment and positive difference ozone content throughout the polar stratosphere in Figure 4c, which shows distributions similar to Figure 3, but for December. It should be noted that there is an increased ozone content during the La Niña phase at altitudes up to 30 km and above 40 km (Figure 4b,d) when analyzing the ozone content in the polar stratosphere in December under conditions of different ENSO phases (without taking into account the QBO). A reduced mixing ratio during the La Niña phase is observed in the range of 30–40 km, which is associated with a weakening of the RMC and, accordingly, a weakening of ozone transport from the tropics. The behavior of the RMC in December remains similar to that in November. According to previous research, the polar stratosphere is traditionally warmer during El Niño [25]. Negative values in the temperature difference (Figure 4b) up to an altitude of approximately 32 km reflect changes in the thermodynamic regime of the polar stratosphere during the winter SSW of 2011–2012 (La Niña-EQBO), which began in late December. The uneven vertical distribution of ozone over the pole with maximum values of the mixing ratio slightly above 30 km, as well as the displacement of the stratospheric polar vortex during the SSW, when averaged over latitude, gives an ambiguous picture of ozone distribution. However, the polar projection shows minimal ozone over the pole under La Niña-EQBO conditions in December (Figure 2i) when averaged over the entire stratosphere.

It is possible to assess the influence of the property of the ozone meridional transport under conditions of different phases without the influence of SSW in the polar stratosphere only in November. Calculations have shown that the meridional transport is significantly weaker in the stratosphere above 35 km under La Niña conditions, regardless of the QBO phase in both November and December. It should also be noted that under La Niña-EQBO conditions, the transport is not only the weakest but also the layer in which higher transfer rates are observed relative to the WQBO (at an altitude of 30 km) is minimal in thickness. The inherent transport under La Niña conditions at altitudes of 25–45 km is parallel to the

surface due to the weaker vertical component of the RMC, while under El Niño conditions, the transport has an arc-shaped structure, which is especially noticeable above 50 km. This transfer should contribute to a greater removal of ozone from the stratosphere to the lower layers of the mesosphere.

In January, the ozone content was still lower under La Niña-EQBO conditions (Figure 2e) relative to other phases despite the major SSW in January 2012 and the abrupt increase in temperature in January 2000. It can be assumed that this is due to the cumulative effect caused by weak ozone transfer from low to high latitudes during La Niña-EQBO. The negative difference in temperature throughout the polar stratosphere and the different signs of ozone increment under the La Niña conditions of the WQBO and EQBO (Figure 5c) are caused by the influence of the SSW, which is clearly visible from the RMC. A similar distribution is observed in Figure 5b; however, the ozone content is significantly higher above the pole under El Niño-WQBO conditions, and it is also valid for El Niño-EQBO (Figure 5d). In January, under El Niño-EQBO conditions, SSWs of varying intensity were observed in all three observed winters. It should also be noted that the boundary between the characteristic ozone distribution in the equatorial belt and the tropical one moves deeper into the Northern Hemisphere to 30° (Figure 5d). Usually, ENSO is in its developed state in January; therefore, the difference of phases' manifestation in atmospheric processes in January and February should be maximum in the tropics. The generation of atmospheric waves in the tropics depends on the phase of ENSO [60,61]. The variability in the activity of planetary waves entering the lower stratosphere is consistent with trends in the ozone content. Therefore, the boundary shift (Figure 5d) may be caused by wave activity in the tropics. The structure of the RMC in January is preserved. Just a weakening of the secondary meridional circulation is noted during the WQBO from the equator to 30° N at an altitude of 30 km (Figure 5b,c).

In February, the effect of the RMC is obscured by the influence of the SSW, which is noticeable in Figure 2e. In winters under El Niño-EQBO conditions, SSWs were most often observed in the second half of January. A large number of SSWs in January and February are also observed under La Niña-WQBO conditions, but the ozone content in the stratosphere is still noticeably lower (Figure 2b). Under El Niño-EQBO conditions, ozone levels reach a maximum by February (Figure 2c) at high latitudes, which is likely due to the fact that SSWs of varying intensities (with and without zonal wind reversal) were observed in all three studied winters (December to February) under El Niño-EQBO conditions. A similar situation, when warming of varying intensity is observed every winter (from December to February), has developed under La Niña-WQBO conditions, but the ozone content in the polar stratosphere is significantly lower than under El Niño-EQBO conditions, which confirms our argument that there is a cumulative effect of weak RMC during La Niña. This effect is noticeable until January inclusive. It is expressed in enhanced transport during La Niña at an altitude of 30 km (from the low ozone area during the EQBO) from the equator towards the pole.

Numerical simulations. Due to the limitation in the duration of reanalysis data in the satellite era, we were able to select only three years from 1979 to the present, which correspond to different combinations of QBO and ENSO during the boreal winter. Therefore, due to strong variability of meteorological fields, the statistical significance of the changes in RMC and temperature we calculated is small in most of the images in Figures 3–5. In this regard, we carried out a series of simulations of global atmospheric circulation using the MUAM model for conditions with four combinations of QBO and ENSO (Figure 6). Ensembles of model solutions consisting of 10 members were considered, with variations between simulated hydrodynamic parameters interpreted as interannual variability [49]. As a result, we obtained temperature and RMC distributions for January similar to those shown in Figure 5.

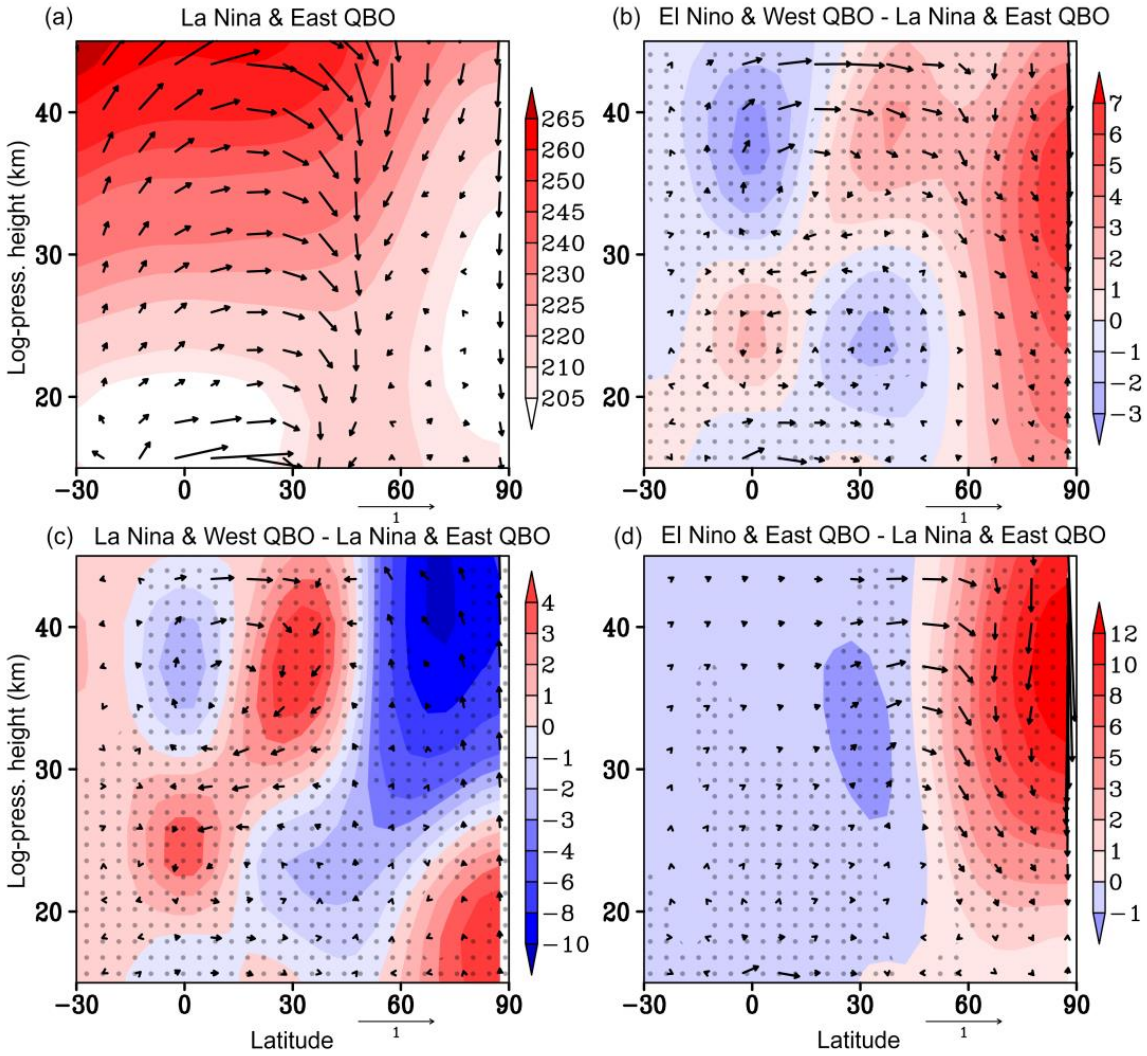

Figure 6. Mean zonal temperature during La Niña-EQBO (**a**) and the difference between La Niña-EQBO and other combinations (**b**–**d**)—shading, mean RMC (**a**), and its increments (**b**–**d**)—arrows, simulated with the MUAM model for January. Dotted areas reveal statistically significant differences in RMC and temperature at 95%.

One can detect a general similarity between the temperature fields (note that in Figure 5, temperature and its anomaly are represented by contours) and the RMC in Figures 5a and 6a, as well as the similarity in their changes in the remaining panels of Figures 5 and 6. In particular, in the equatorial region, the change in the QBO phase in Figures 5b,c and 6b,c manifests itself in cooling and strengthening of upward flows above 30 km and warming and weakening of upward flows below 30 km. In combination with poleward increments of the RMC in the tropical region, in the altitude range of 35–45 km and with reverse processes at 25–35 km, the secondary meridional circulation cells discussed above are formed. This, in turn, is accompanied by warming of the upper and cooling of the lower stratosphere at 20–40° north, respectively. In the high-latitude stratosphere, there are warming trends during El-WQBO (Figure 6b) and cooling during La-WQBO (Figure 5c). However, there are also discrepancies between temperature and RMC, noticeable, in particular, in the subpolar region in Figures 5b and 6b. This is due to the pronounced influence of SSW in the reanalysis data, whereas in modeling, the SSW statistics are more uniform for different combinations. If we compare Figures 5d and 6d, estimating the influence of ENSO with the same QBO phase, the temperature changes in both cases in the tropical stratosphere are small, and the changes in the RMC in the reanalysis data are enhanced above 35 km, which is not observed in the simulation results.

This effect is probably explained by a change in wave activity caused by the influence of the SSW. In the extratropical region in Figures 5d and 6d, there is a similarity expressed through the warming of the stratosphere during El Niño and the strengthening of the descending branch of the RMC.

Numerical modeling allowed us to achieve the required level of statistical significance and confirm the existence of the considered trends in temperature and residual circulation caused by natural tropical stratospheric oscillations.

4. Conclusions

The study examines the influence of RMC on ozone content in the polar stratosphere during boreal winter under different phases of ENSO and QBO:

- the different vertical distribution of ozone in the equatorial stratosphere, as well as the strengthening/weakening of the secondary meridional circulation in the tropics, are highly dependent on the QBO phase;
- under El Niño conditions, the amplification of the RMC from the tropical to the polar stratosphere is stronger at altitudes where ozone is more abundant in the tropics;
- the RMC modification and intensification are observed from ozone-depleted areas under La Niña conditions;
- a "cumulative" effect is observed by February under La Niña conditions and the easterly QBO, which is expressed in the lowest ozone content in the polar stratosphere;
- the numerical experiments carried out using the MUAM confirmed tendencies in changes in the meridional transport detected from the reanalysis data for different combinations of QBO and ENSO.

Three winter seasons for each ENSO-QBO combination were selected and analyzed using MERRA2 reanalysis data. The winters during the ENSO neutral phase, as well as winters under conditions of the QBO phase changing, were not considered. It has been demonstrated that the nature of the RMC is different under El Niño and La Niña conditions. The transfer from the tropical to the polar stratosphere during a positive El Niño phase is stronger in the tropics relative to La Niña at altitudes where ozone content is higher. The nature of transfer contributes to the ozone removal into the mesosphere's lower layers, which is associated with the stronger vertical RMC component under El Niño. During the negative phase of ENSO (La Niña), transport is parallel to the surface, and its enhancement is observed in layers with low ozone content in the tropical stratosphere.

The horizontal distributions of ozone content in the stratosphere in the Northern Hemisphere were considered. In November, minimum values of ozone mixing ratio are observed under La Niña-EQBO conditions over the North Pole, Canada, and the Far East. The changes are of the order of 10%. In December, negative ozone anomaly during La Niña-EQBO moves toward Eurasia and the Atlantic. In January and February, the differences in overall ozone trends associated with the QBO dominate. There is an increase in ozone during WQBO compared to the EQBO over the North Atlantic and Europe in January and over Canada in February.

The phases of ENSO influence the nature of the transport, which is reflected in its strengthening/weakening at different heights and shapes (flat or arched structures). The QBO phase is manifested in different ozone distributions in the equatorial stratosphere, as well as in the strengthening/weakening of the secondary meridional circulation in the tropics. This adds up to different ozone content in the polar stratosphere. The ozone responses to ENSO and QBO can largely cancel out or enhance each other depending on their relative phases and magnitudes. Thus, estimates of natural ozone variability must take into account both the QBO and ENSO phases [62].

The manifestation of the QBO in the ozone content in the equatorial and tropical regions is clearly seen in November. The positive changes during the WQBO are observed over the equator, and negative ones are situated at the latitude belt between 15° and 25° in both hemispheres. The observed RMC and temperature anomalies shown in Figure 3b,c, leading to changes in ozone content in the equatorial and tropical regions, are

explained by the influence of the secondary meridional circulation, which is induced by the QBO. Such secondary meridional circulation cells are characterized by adiabatic heating/cooling due to vertical movements in areas of zonal wind shear, causing corresponding temperature anomalies.

In December, there is an increased ozone content during the La Niña phase at altitudes up to 30 km and above 40 km in the polar stratosphere. A reduced mixing ratio during the La Niña in the range of 30–40 km is associated with a weakening of the RMC and, accordingly, a weakening of ozone transport from the tropics. The QBO-associated changes in RMC and ozone content in December are basically similar to those in November. The uneven vertical distribution of ozone over the pole with maximum values of the mixing ratio slightly above 30 km, as well as disturbances caused by the SSW, give an ambiguous picture of ozone distribution changes over the Pole in December. However, the polar projection shows minimal ozone under La Niña-EQBO conditions in the entire stratosphere.

Due to different RMC under the conditions of La Niña and the easterly QBO, a "cumulative" effect is observed by February, which is expressed in the lowest ozone content in the polar stratosphere in comparison with other tropical oscillations' combinations. SSWs of varying intensity were observed in almost every studied winter. The contribution of every individual SSW to the ozone content is almost impossible to estimate. It is worth noting that in winters under La Niña-EQBO conditions, major SSWs were also observed. However, no noticeable increase in ozone content compared to other combinations was observed due to weak RMC.

Due to the limitation of the duration of reanalysis data in the satellite era, we were only able to select three years from 1979 to the present that correspond to different combinations of QBO and ENSO during the boreal winter. The numerical modeling of the thermodynamic structure of the stratosphere for different ENSO-QBO combinations made it possible to consider statistically significant increments of the RMC and temperature caused by changes in the considered phases and verify the trends in changes in dynamic processes in the atmosphere observed from the reanalysis. The advantage of numerical modeling in this case was that we could consider the effect of changes in the phases of tropical oscillations in its pure form without taking into account additional factors associated with the stratospheric variability. In addition, modeling allows us to overcome the main drawback of reanalysis data—the short time interval available for research, which does not allow for achieving sufficient statistical significance. We were able to show that the general trends in circulation changes, calculated for groups of three years for each combination according to the reanalysis data, coincide with the modeling results, which confirms the adequacy and reliability of the results obtained.

The obtained results, which concern the ENSO anomalies on ozone, are in good agreement with the results shown in [63]. The comparison with other investigations on the QBO and ozone anomalies demonstrates some contradiction mostly because of different methods of the QBO phase determination [64].

The state of the ozone layer has recently attracted public attention due to the noted trends in its global content decrease since the end of the XX century and the understanding of its role not only as a protector of life on Earth from the harmful effects of the hard part of ultraviolet radiation from the Sun but also as a factor influencing climate and the biosphere as a whole. In this regard, the main attention of society is drawn to the influence of various factors, dynamic and anthropogenic in nature, affecting the state of the ozone layer. The results obtained in the study can be used in seasonal forecasting of the thermodynamic regime of the polar stratosphere since ozone contributes to air heating, as well as in the seasonal ozone projections.

Supplementary Materials: The following supporting information can be downloaded at: https://www.mdpi.com/article/10.3390/atmos15060717/s1, Figure S1: Mean zonal ozone mixing ratio (MLS, left panels), (MERRA2, right panels), for November 2009 (top panels), November 2017 (lower panels); Figure S2: Mean zonal ozone mixing ratio (MLS, left panels), (MERRA2, right panels), for December 2007 (top panels), January 2011 (lower panels); Figure S3: Averaged RMC (arrows) for different ENSO-QBO phases; vertical componet (shading) for November; Figure S4: Averaged RMC (arrows) for different ENSO-QBO phases; vertical componet (shading) for December; Figure S5: Latitude-height distributions of mean zonal ozone mixing ratio increments relative to the La Niña-EQBO phases for (a)—El Niño-WQBO; (b)—La Niña-EQBO; (c)—El Niño-EQBO for November. Shaded areas reveal statistically insignificant differences at 95%; Figure S6: Latitude-height distributions of mean zonal ozone mixing ratio increments relative to the La Niña-EQBO phases for (a)—El Niño-WQBO; (b)—La Niña-EQBO; (c)—El Niño-EQBO for December. Shaded areas reveal statistically insignificant differences at 95%; Figure S7: Latitude-height distributions of mean zonal ozone mixing ratio increments relative to the La Niña-EQBO phases for (a)—El Niño-WQBO; (b)—La Niña-EQBO; (c)—El Niño-EQBO for January. Shaded areas reveal statistically insignificant differences at 95%.

Author Contributions: Conceptualization, T.E. and A.K.; methodology, T.E.; software, A.K.; validation, O.A. and A.O.; formal analysis, K.D.; investigation, T.E.; data curation, T.E.; writing—original draft preparation, T.E. and A.K.; writing—review and editing, K.D. and A.O.; visualization, O.A.; project administration, A.K.; funding acquisition, A.K. All authors have read and agreed to the published version of the manuscript.

Funding: Calculation of residual circulation and performing numerical simulations were supported by the Russian Science Foundation: grant #20-77-10006-P (https://rscf.ru/en/project/20-77-10006/); processing reanalysis data and statistical analysis were supported by Saint Petersburg University (research grant 116234986).

Institutional Review Board Statement: Not applicable.

Informed Consent Statement: Not applicable.

Data Availability Statement: The MERRA-2 dataset can be obtained from https://disc.gsfc.nasa.gov/datasets/M2I6NVANA_5.12.4/summary (accessed on 28 April 2022). All source codes for computing RMC can be accessed from the corresponding author upon request. Plots in this study were made using Grid Analysis and Display System (GrADS), which is a free software developed by the NASA Advanced Information Systems Research Program.

Acknowledgments: The reanalysis data were provided by MERRA-2, the National Aeronautics and Space Administration (NASA).

Conflicts of Interest: The authors declare no conflicts of interest.

References

1. Newman, P.A.; Oman, L.D.; Douglass, A.R.; Fleming, E.L.; Frith, S.M.; Hurwitz, M.M.; Kawa, S.R.; Jackman, C.H.; Krotkov, N.A.; Nash, E.R.; et al. What would have happened to the ozone layer if chlorofluorocarbons (CFCs) had not been regulated? *Atmos. Chem. Phys.* **2009**, *9*, 2113–2128. [CrossRef]
2. Newchurch, M.J.; Sun, D.; Kim, J.H.; Liu, X. Tropical tropospheric ozone derived using Clear-Cloudy Pairs (CCP) of TOMS measurements. *Atmos. Chem. Phys.* **2003**, *3*, 683–695. [CrossRef]
3. Barnes, E.A.; Hurrell, J.W.; Ebert-Uphoff, I.; Anderson, C.; Anderson, D. Viewing Forced Climate Patterns Through an AI Lens. *Geophys. Res. Lett.* **2019**, *46*, 13389–13398. [CrossRef]
4. World Meteorological Organization (WMO). Executive Summary. In *Scientific Assessment of Ozone Depletion*; GAW Report No. 278; WMO: Geneva, Switzerland, 2022; p. 56.
5. Clarmann, V.T. Chlorine in the stratosphere. *Atmosfera* **2013**, *26*, 415–458. [CrossRef]
6. Harrison, J.J.; Chipperfield, M.P.; Hossaini, R.; Boone, C.D.; Dhomse, S.; Feng, W.; Bernath, P.F. Phosgene in the upper troposphere and lower stratosphere: A marker for product gas injection due to chlorine-containing very short-lived substances. *Geophys. Res. Lett.* **2019**, *46*, 1032–1039. [CrossRef]
7. Bednarz, E.M.; Hossaini, R.; Chipperfield, M.P. Atmospheric impacts of chlorinated very short-lived substances over the recent past—Part 2: Impacts on ozone. *Atmos. Chem. Phys.* **2023**, *23*, 13701–13711. [CrossRef]
8. Chipperfield, M. Atmospheric science: Nitrous oxide delays ozone recovery. *Nat. Geosci.* **2009**, *2*, 742–743. [CrossRef]
9. Wang, W.; Tian, W.; Dhomse, S.; Xie, F.; Shu, J.; Austin, J. Stratospheric ozone depletion from future nitrous oxide increases. *Atmos. Chem. Phys.* **2014**, *14*, 12967–12982. [CrossRef]

10. Dietmüller, S.; Garny, H.; Eichinger, R.; Ball, W.T. Analysis of recent lower stratospheric ozone trends in chemistry climate models. *Atmos. Chem. Phys.* **2021**, *21*, 6811–6837. [CrossRef]
11. Li, Y.; Dhomse, S.S.; Chipperfield, M.P.; Feng, W.; Bian, J.; Xia, Y.; Guo, D. Quantifying stratospheric ozone trends over 1984–2020: A comparison of ordinary and regularized multivariate regression models. *Atmos. Chem. Phys.* **2023**, *23*, 13029–13047. [CrossRef]
12. Egorova, T.; Sedlacek, J.; Sukhodolov, T.; Karagodin-Doyennel, A.; Zilker, F.; Rozanov, E. Montreal Protocol's impact on the ozone layer and climate. *Atmos. Chem. Phys.* **2023**, *23*, 5135–5147. [CrossRef]
13. Zvyagintsev, A.M.; Vargin, P.N.; Peshin, S. Total ozone variations and trends during the period 1979–2014. *Atmos. Ocean. Opt.* **2015**, *28*, 575–584. [CrossRef]
14. Solomon, S.; Ivy, D.J.; Kinnison, D.; Mills, M.J.; Neely, R.; Schmidt, A. Emergence of healing in the Antarctic ozone layer. *Atmos. Ocean.* **2016**, *353*, 269–274. [CrossRef] [PubMed]
15. Chipperfield, M.P.; Bekki, S.; Dhomse, S.S.; Harris, N.R.P.; Hassler, B.; Hossaini, R.; Steinbrecht, W.; Thiéblemont, R.; Weber, M. Detecting recovery of the stratospheric ozone layer. *Nature* **2017**, *549*, 211–218. [CrossRef] [PubMed]
16. Nath, O.; Sridharan, S.; Gadhavi, H. Equatorial stratospheric thermal structure and ozone variations during the sudden stratospheric warming of 2013. *J. Atmos. Sol. Terr. Phys.* **2015**, *122*, 129–137. [CrossRef]
17. Nikulin, G.; Karpechko, A. The mean meridional circulation and midlatitude ozone buildup. *Atmos. Chem. Phys.* **2005**, *5*, 3159–3172. [CrossRef]
18. Weber, M.; Dikty, S.; Burrows, J.P.; Garny, H.; Dameris, M.; Kubin, A.; Abalichin, J.; Langematz, U. The Brewer-Dobson circulation and total ozone from seasonal to decadal time scales. *Atmos. Chem. Phys.* **2011**, *11*, 11221–11235. [CrossRef]
19. Blessmann, D.; Wohltmann, I.; Rex, M. Influence of transport and mixing in autumn on stratospheric ozone variability over the Arctic in early winter. *Atmos. Chem. Phys.* **2012**, *12*, 7921–7930. [CrossRef]
20. Polyakov, A.; Virolainen, Y.; Nerobelov, G.; Kozlov, D.; Timofeyev, Y. Six Years of IKFS-2 Global Ozone Total Column Measurements. *Remote Sens.* **2023**, *15*, 2481. [CrossRef]
21. Garfinkel, C.I.; Hartmann, D.L. Effects of the El Niño–Southern Oscillation and the Quasi-Biennial Oscillation on polar temperatures in the stratosphere. *J. Geophys. Res.* **2007**, *112*, D19112. [CrossRef]
22. Dijkstra, H.A. The ENSO phenomenon: Theory and mechanisms. *Adv. Geosci.* **2006**, *6*, 3–15. [CrossRef]
23. Trenberth, K.E. The Definition of El Niño. *Bull. Am. Meteorol. Soc.* **1997**, *78*, 2771–2778. [CrossRef]
24. Wang, C.; Deser, C.; Yu, J.Y.; DiNezio, P.; Clement, A. El Niño and Southern Oscillation (ENSO): A Review. In *Coral Reefs of the Eastern Tropical Pacific*; Springer: Dordrecht, The Netherlands, 2016; Volume 8, pp. 85–106. [CrossRef]
25. Butler, A.H.; Polvani, L.M. El Niño, La Niña, and stratospheric sudden warmings: A reevaluation in light of the observational record. *Geophys. Res. Lett.* **2011**, *38*, L13807. [CrossRef]
26. Ermakova, T.S.; Aniskina, O.G.; Statnaia, I.A.; Motsakov, M.A.; Pogoreltsev, A.P. Simulation of the ENSO influence on the extra-tropical middle atmosphere. *Earth Planets Space* **2019**, *71*, 8. [CrossRef]
27. Holton, J.R.; Tan, H.C. The Influence of the Equatorial Quasi-Biennial Oscillation on the Global Circulation at 50 mb. *J. Atmos. Sci.* **1980**, *37*, 2200–2208. [CrossRef]
28. Koval, A.V.; Gavrilov, N.M.; Pogoreltsev, A.I.; Efimov, M.M. Modeling Residual Meridional Circulation at Different Phases of the Quasi-Biennial Oscillation. *Atmos. Ocean. Phys.* **2022**, *58*, 22–29. [CrossRef]
29. Kumar, V.; Yoden, S.; Hitchman, M.H. QBO and ENSO Effects on the Mean Meridional Circulation, Polar Vortex, Subtropical Westerly Jets, and Wave Patterns During Boreal Winter. *J. Geophys. Res. Atmos.* **2022**, *127*, e2022JD036691. [CrossRef]
30. Xuan, M.; Wang, L.; Smith, D.; Hermanson, L.; Eade, R.; Dunstone, N.; Hardiman, S.; Zhang, J. ENSO and QBO modulation of the relationship between Arctic sea ice loss and Eurasian winter climate. *Environ. Res. Lett.* **2022**, *17*, 124016. [CrossRef]
31. Gelaro, R.; McCarty, W.; Suarez, M.J. The Modern-Era Retrospective Analysis for Research and Applications, Version 2 (MERRA-2). *J. Clim.* **2017**, *30*, 5419–5454. [CrossRef]
32. Rienecker, M.M.; Suarez, M.J.; Todling, R.; Bacmeister, J.; Takacs, L.; Liu, H.-C.; Gu, W.; Sienkiewicz, M.; Koster, R.D.; Gelaro, R.; et al. The GEOS-5 Data Assimilation System—Documentation of Versions 5.0.1 and 5.1.0, and 5.2.0. Available online: https://ntrs.nasa.gov/citations/20120011955 (accessed on 10 June 2024).
33. Lubis, S.W.; Silverman, V.; Matthes, K.; Harnik, N.; Omrani, N.-E.; Wahl, S. How does downward planetary wave coupling affect polar stratospheric ozone in the Arctic winter stratosphere? *Atmos. Chem. Phys.* **2017**, *17*, 2437–2458. [CrossRef]
34. Albers, J.R.; Perlwitz, J.; Butler, A.H.; Birner, T.; Kiladis, G.N.; Lawrence, Z.D.; Manney, G.L.; Langford, A.O.; Dias, J. Mechanisms governing interannual variability of stratosphere-to-troposphere ozone transport. *J. Geophys. Res. Atmos.* **2018**, *123*, 234–260. [CrossRef]
35. Wargan, K.; Labow, G.; Frith, S.; Pawson, S.; Livesey, N.; Partyka, G. Evaluation of the ozone fields in NASA's MERRA-2 reanalysis. *J. Clim.* **2017**, *30*, 2961–2988. [CrossRef] [PubMed]
36. Schranz, F.; Hagen, J.; Stober, G.; Hocke, K.; Murk, A.; Kämpfer, N. Small-scale variability of stratospheric ozone during the sudden stratospheric warming 2018/2019 observed at Ny-Ålesund, Svalbard. *Atmos. Chem. Phys.* **2020**, *20*, 10791–10806. [CrossRef]
37. Hong, H.-J.; Reichler, T. Local and remote response of ozone to Arctic stratospheric circulation extremes. *Atmos. Chem. Phys.* **2021**, *21*, 1159–1171. [CrossRef]

38. Bahramvash Shams, S.; Walden, V.P.; Hannigan, J.W.; Randel, W.J.; Petropavlovskikh, I.V.; Butler, A.H.; de la Cámara, A. Analyzing ozone variations and uncertainties at high latitudes during sudden stratospheric warming events using MERRA-2. *Atmos. Chem. Phys.* **2022**, *22*, 5435–5458. [CrossRef]
39. Ermakova, T.S.; Koval, A.V.; Smyshlyaev, S.P.; Didenko, K.A.; Aniskina, O.G.; Savenkova, E.N.; Vinokurova, E.V. Manifestations of Different El Niño Types in the Dynamics of the Extratropical Stratosphere. *Atmosphere* **2022**, *13*, 2111. [CrossRef]
40. Hitchman, M.H.; Yoden, S.; Haynes, P.H.; Kumar, V.; Tegtmeier, S. An Observational History of the Direct Influence of the Stratospheric Quasi-biennial Oscillation on the Tropical and Subtropical Upper Troposphere and Lower Stratosphere. *J. Meteorol. Soc. Jpn. Ser. II* **2021**, *99*, 239–267. [CrossRef]
41. Kobayashi, S.; Ota, Y.; Harada, H. The JRA-55 Reanalysis: General Specifications and Basic Characteristics. *J. Meteorol. Soc. Jpn.* **2015**, *93*, 5–48. [CrossRef]
42. Charney, J.G.; Drazin, P.G. Propagation of Planetary-Scale Disturbances from the Lower into the Upper Atmosphere. *J. Geophys. Res.* **1961**, *66*, 83–109. [CrossRef]
43. Holton, J.R. *An Introduction to Dynamic Meteorology*, 4th ed.; Elsevier Academic Press: Amsterdam, The Netherlands, 2004; 535p.
44. Butchart, N. The Brewer-Dobson circulation. *Rev. Geophys.* **2014**, *52*, 157–184. [CrossRef]
45. Andrews, D.G.; McIntyre, M.E. Planetary Waves in Horizontal and Vertical Shear: The Generalized Eliassen-Palm Relation and the Mean Zonal Acceleration. *J. Atmos. Sci.* **1976**, *33*, 2031–2048. [CrossRef]
46. Koval, A.V.; Chen, W.; Didenko, K.A.; Ermakova, T.S.; Gavrilov, N.M.; Pogoreltsev, A.I.; Toptunova, O.N.; Wei, K.; Yarusova, A.N.; Zarubin, A.S. Modelling the residual mean meridional circulation at different stages of sudden stratospheric warming events. *Ann. Geophys.* **2021**, *39*, 357–368. [CrossRef]
47. de la Cámara, A.; Abalos, M.; Hitchcock, P.; Calvo, N.; Garcia, R.R. Response of Arctic ozone to sudden stratospheric warmings. *Atmos. Chem. Phys.* **2018**, *18*, 16499–16513. [CrossRef]
48. Denton, M.H.; Kivi, R.; Ulich, T.; Rodger, C.J.; Clilverd, M.A.; Denton, J.S.; Lester, M. Observed response of stratospheric and mesospheric composition to sudden stratospheric warmings. *J. Atmos. Sol.-Terr. Phys.* **2019**, *191*, 10505. [CrossRef]
49. Veenus, V.; Das, S.S.; David, L.M. Ozone Changes Due To Sudden Stratospheric Warming-Induced Variations in the Intensity of Brewer-Dobson Circulation: A Composite Analysis Using Observations and Chemical-Transport Model. *Geophys. Res. Lett.* **2023**, *50*, e2023GL103353. [CrossRef]
50. Pogoreltsev, A.I.; Vlasov, A.A.; Fröhlich, K.; Jacobi, C. Planetary waves in coupling the lower and upper atmosphere. *J. Atmos. Sol.-Terr. Phys.* **2007**, *69*, 2083–2101. [CrossRef]
51. Koval, A.V.; Gavrilov, N.M.; Pogoreltsev, A.I.; Kandieva, K.K. Dynamical impacts of stratospheric QBO on the global circulation up to the lower thermosphere. *J. Geophys. Res. Atmos.* **2022**, *127*, e2021JD036095. [CrossRef]
52. Nagashima, T.; Takahashi, M.; Fumio, H. The first simulation of an ozone QBO in a general circulation model. *Geophys. Res. Lett.* **1998**, *25*, 3131–3134. [CrossRef]
53. Butchart, N.; Scaife, A.A.; Austin, J.; Hare, S.H.E.; Knight, J.R. Quasi-biennial oscillation in ozone in a coupled chemistry-climate model. *J. Geophys. Res. Atmos.* **2003**, *108*, 4486. [CrossRef]
54. Chipperfield, M.; Gray, L.; Kinnersley, J.; Zawodny, J. A two-dimensional model study of the QBO signal in SAGE II NO_2 and O_3. Geophys. *Res. Lett.* **1994**, *21*, 589–592. [CrossRef]
55. Tian, W.; Chipperfield, M.P.; Gray, L.J.; Zawodny, J.M. Quasi-biennial oscillation and tracer distributions in a coupled chemistry-climate model. *J. Geophys. Res. Atmos.* **2006**, *111*, D20301. [CrossRef]
56. Fioletov, V.E. Ozone climatology, trends, and substances that control ozone. *Atmos.-Ocean* **2008**, *46*, 39–67. [CrossRef]
57. Dickinson, R.E. Planetary Rossby waves propagating vertically through weak westerly wave guides. *J. Atmos. Sci.* **1968**, *25*, 984–1002. [CrossRef]
58. Choi, W.; Lee, H.; Grant, W.B.; Park, J.H.; Holton, J.R.; Lee, K.M.; Naujokat, B. On the secondary meridional circulation associated with the quasi-biennial oscillation. *Tellus B Chem. Phys. Meteorol.* **2002**, *54*, 395–406. [CrossRef]
59. Ribera, P.; Pena-Ortiz, C.; Garcia-Herrera, R.; Gallego, D.; Gimeno, L.; Hernandez, E. Detection of the secondary meridional circulation associated with the quasi-biennial oscillation. *J. Geophys. Res.* **2004**, *109*, D18112. [CrossRef]
60. Rakhman, S.; Lubis, S.W.; Setiawan, S. Impact of ENSO on seasonal variations of Kelvin Waves and mixed Rossby-Gravity Waves. *IOP Conf. Ser. Earth Environ. Sci.* **2017**, *54*, 012035. [CrossRef]
61. Randel, W.J.; Wu, F.; Stolarski, R. Changes in Column Ozone Correlated with the Stratospheric EP Flux. *J. Meteorol. Soc. Jpn.* **2002**, *80*, 849–862. [CrossRef]
62. Olsen, M.; Manney, G.; Liu, J. The ENSO and QBO Impact on Ozone Variability and Stratosphere-Troposphere Exchange Relative to the Subtropical Jets. *J. Geophys. Res. Atmos.* **2019**, *124*, 7379–7392. [CrossRef]
63. Benito-Barca, S.; Calvo, N.; Abalos, M. Driving mechanisms for the El Niño–Southern Oscillation impact on stratospheric ozone, Atmos. *Chem. Phys.* **2022**, *22*, 15729–15745. [CrossRef]
64. Zhang, J.; Zhang, C.; Zhang, K.; Xu, M.; Duan, J.; Chipperfield, M.P.; Feng, W.; Zhao, S.; Xie, F. The role of chemical processes in the quasi-biennial oscillation (QBO) signal in stratospheric ozone. *Atmos. Environ.* **2021**, *224*, 117906. [CrossRef]